Electronic Supplementary Material (ESI) for Journal of Materials Chemistry B.

Supplementary Information

for

Inflammatory-stimuli-responsive turn-on NIR fluorogenic theranostic prodrug: adjuvant delivery of diclofenac and hydrogen sulfide attenuates acute inflammatory disorders

Contents

Synthesis of the by-product 13a

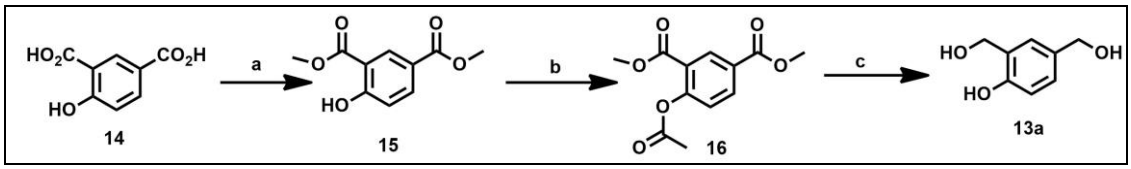

Scheme 1. Synthetic scheme to compound **13a**. Reagents and conditions: (a) Methanol, DCC, DMAP, dry DCM, 0 °C - RT, 5 h; (b) Acetyl chloride, pyridine, dry DCM, 0 °C - RT, 6 h; (c) $LiAlH_4$, dry THF, 0 °C - RT, 14 h.

Synthesis of compound 15[1]

Compound **15** was synthesized following the literature procedure with a minor modifications.[2] To a mixture of 4-hydroxyisophthalic acid **14** (0.10 g, 0.55 mmol) and DMAP (7.00 mg, 0.06 mmol) was added dry DCM (3 mL) under an inert atmosphere. Methanol (0.09 mL, 2.20 mmol) was added to the reaction mixture and cooled to 0 °C. A solution of DCC in dry DCM (3 mL) was added under inert conditions at 0 °C. The reaction mixture was slowly brought to room temperature and stirred for 5 h. The progress of the reaction was monitored by TLC analysis. Upon completion, the reaction mixture was diluted with DCM and washed with water (3 × 5 mL). The organic layer was dried over anhydrous sodium sulfate, the solvent was evaporated under reduced pressure, and the crude compound was purified by silica gel (100-200 mesh) column chromatography using 20% ethyl acetate in pet. ether as a mobile phase to afford the pure product **15** as a light brown solid. R_f = 0.7 (20% ethyl acetate in pet. ether); yield: 0.11 g (90%). ^{1}H NMR (400 MHz, $CDCl_3$) δ (ppm) = 11.21 (s, 1H), 8.57 (s, 1H), 8.12 (d, *J* = 5.6 Hz, 1H), 7.02 (d, *J* = 5.6 Hz, 1H), 3.99 (s, 3H), 3.91 (s, 3H). ^{13}C NMR (150 MHz, $CDCl_3$) δ (ppm) = 169.1, 165.0 164.1, 135.6, 131.5, 120.4, 116.8, 111.1, 51.6, 51.1.

Synthesis of compound 16[1]

Compound **16** was synthesized following the literature method with a minor modifications.[3] To a stirred solution of compound **15** (0.05 g, 0.24 mmol) in dry DCM (3 mL) was added pyridine (0.04 mL, 0.48 mmol) under an inert atmosphere and cooled to 0 °C. After 10 min, acetyl chloride (0.03 mL, 0.48 mmol) was added dropwise. The reaction mixture was slowly brought to room temperature and stirred for 6 h. The progress of the reaction was monitored by TLC analysis. Upon completion, the organic solvent was evaporated under reduced pressure and the crude compound was purified by silica gel (100-200 mesh) column chromatography using 20% ethyl acetate in pet. ether as a mobile phase to afford the pure product **16** as a colourless liquid.

R_f = 0.5 (20% ethyl acetate in pet. ether); yield: 0.04 g (66%). ^{1}H NMR (400 MHz, $CDCl_3$) δ (ppm) = 8.68 (d, J = 2.2 Hz, 1H), 8.22 (dd, J_1 = 8.4 Hz, J_2 = 2.2 Hz, 1H), 7.19 (d, J = 8.4 Hz, 1H), 3.94 (s, 3H), 3.90 (s, 3H), 2.37 (s, 3H). ^{13}C NMR (150 MHz, $CDCl_3$) δ (ppm) = 168.2, 164.5, 163.1, 153.1, 133.9, 132.3, 127.1, 123.2, 122.3, 51.5, 51.4, 19.9.

Synthesis of compound 13a[1]

The compound **13a** was synthesized following the literature procedure with slight modifications.[4] To a stirred solution of compound **16** (0.05 g, 0.20 mmol) in dry THF (4 mL) was added lithium aluminium hydride (LAH) (0.08 g, 2.00 mmol) at 0 °C under an inert atmosphere. The reaction mixture was allowed to attain room temperature and stirred for 14 h. The progress of the reaction was monitored by TLC analysis. Upon completion, 2N HCl (5 mL) was added slowly to the reaction mixture at ice-cold conditions to quench the reaction. The solvent was evaporated under reduced pressure and the residue was extracted with ethyl acetate. The organic layer was dried over anhydrous sodium sulfate, the solvent was evaporated under reduced pressure, and the crude compound was purified by silica gel (100-200 mesh) column chromatography using 70% ethyl acetate in pet. ether as a mobile phase to afford the pure product **13a** as a light brown liquid. R_f = 0.4 (70% ethyl acetate in pet. ether); yield: 0.02 g (64%). ^{1}H NMR (400 MHz, CD_3OD) δ (ppm) = 7.26 (d, J = 2.3 Hz, 1H), 7.09 (dd, J_1 = 8.1 Hz, J_2 = 2.3, 1H), 6.74 (d, J = 8.2, 1H), 4.64 (s, 2H), 4.49 (s, 2H). ^{13}C NMR (150 MHz, CD_3OD) δ (ppm) = 155.9, 133.6, 129.0, 128.9, 128.8, 116.0, 65.5, 61.3.

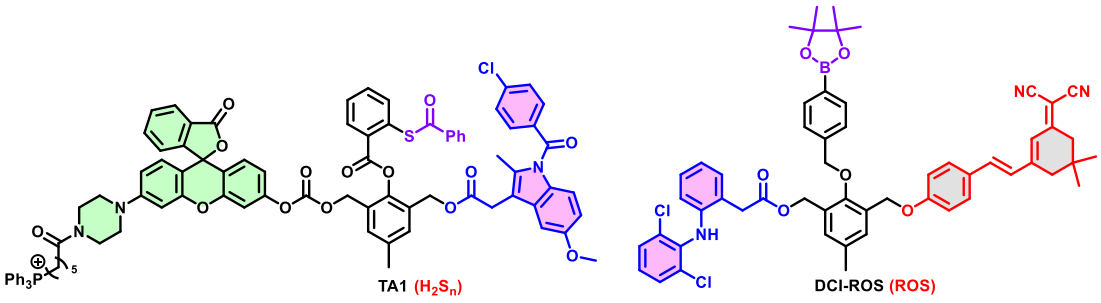

Figure S1. Chemical structures of the turn-on fluorogenic prodrugs of NSAIDs (**TA1** and **DCI-ROS**). The triggering bio-analyte is highlighted in the parenthesis, besides the names of the prodrugs.

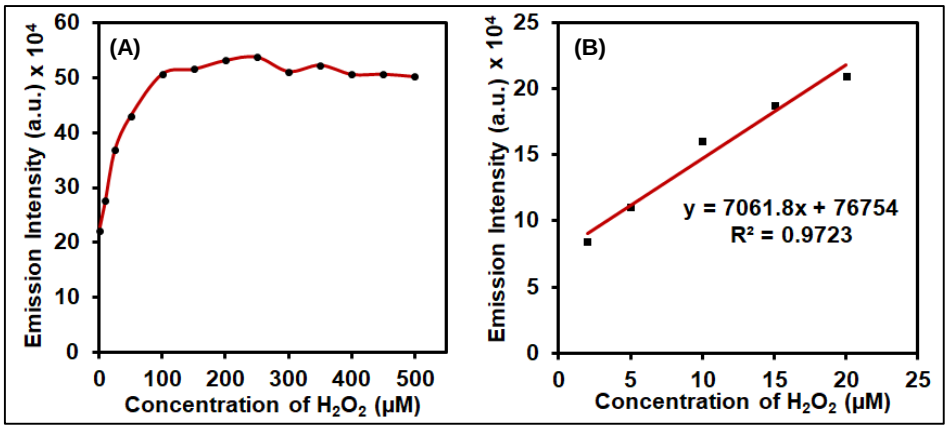

Figure S2. (A) Emission spectra of **DCF-HS** (5 μM) at 655 nm with varying concentration of H_2O_2 (0 - 500 μM); (B) Emission spectra of **DCF-HS** (5 μM) with variable concentration of H_2O_2 (0 - 20 μM) and with a fixed incubation time of 10 h for calculating the LOD of **DCF-HS** towards H_2O_2.

Table S1. Calculation of standard deviation (σ) of blank measurements of **DCF-HS** (5 μM).

Entry	Emission Intensity (a.u.) at 655 nm	Entry	Emission Intensity (a.u.) at 655 nm
1	116428.8	6	114219.3
2	118941	7	119912.5
3	115221.9	8	114553.3
4	111025.9	9	116177.6
5	110218	10	114131.3
Mean = 115083		SD (σ) = 2886.139	

LOD = 3σ/K = 3×2886.13/7061.8 = 1.2 μM

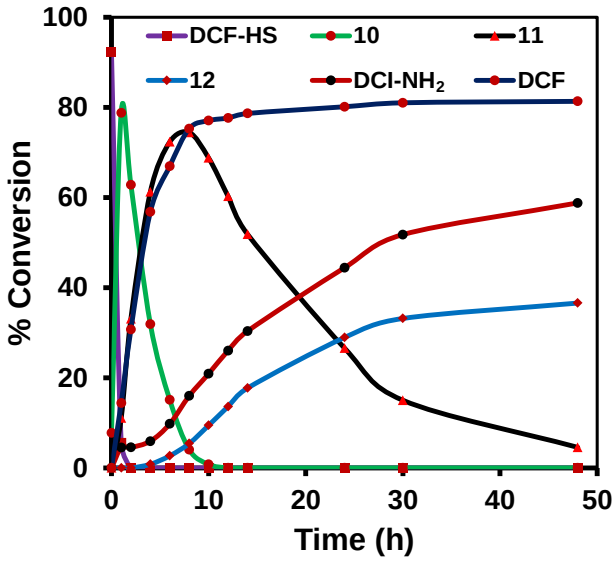

Figure S3. Progress of the reaction of **DCF-HS** (50 µM) with H_2O_2 (2 mM) over 48 h. Relative peak areas of compounds such as **DCF-HS**, **10**, **11**, **12**, **DCF**, and **DCI-NH$_2$** in the reaction mixture were monitored to determine %conversion. The peak area of **DCF-HS**, **10**, **11**, **12**, and **DCI-NH$_2$** were measured at 400 nm, and the peak area of **DCF** was measured at 280 nm.

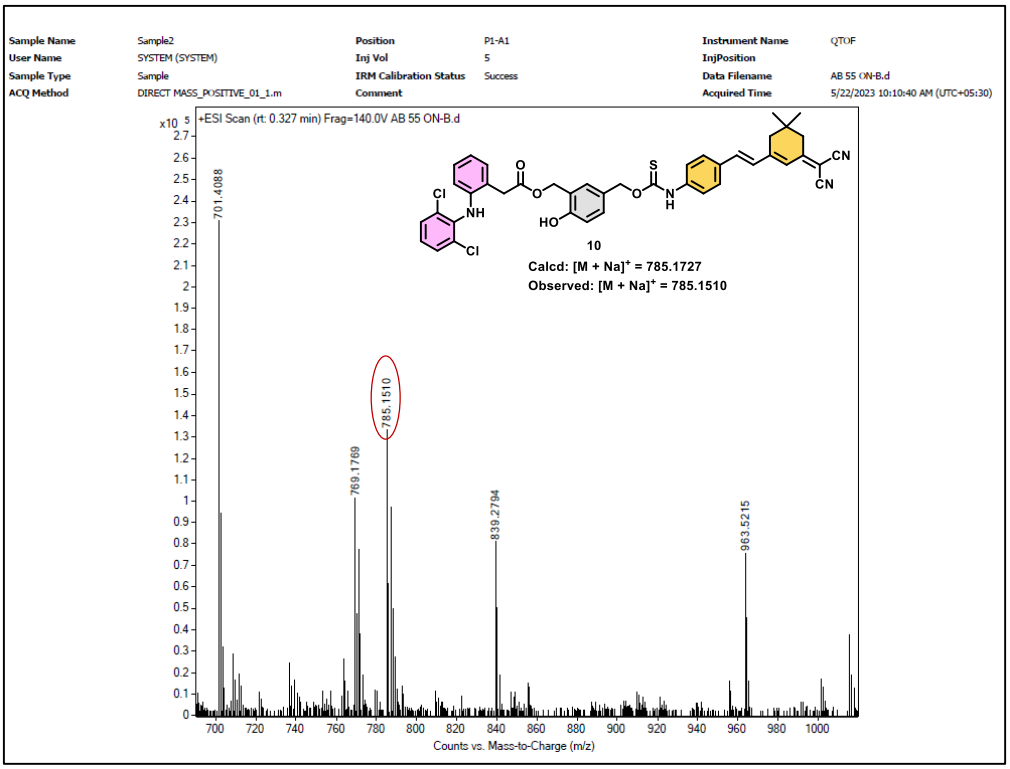

Figure S4. ESI-MS spectrum of the intermediate **10** in the reaction mixture of prodrug **DCF-HS** with H_2O_2 during HPLC analysis. ESI-MS (+ve) *m/z* calcd for $C_{42}H_{36}Cl_2N_4NaO_4S$ $[M + Na]^+$ = 785.1727; obs = 785.1510.

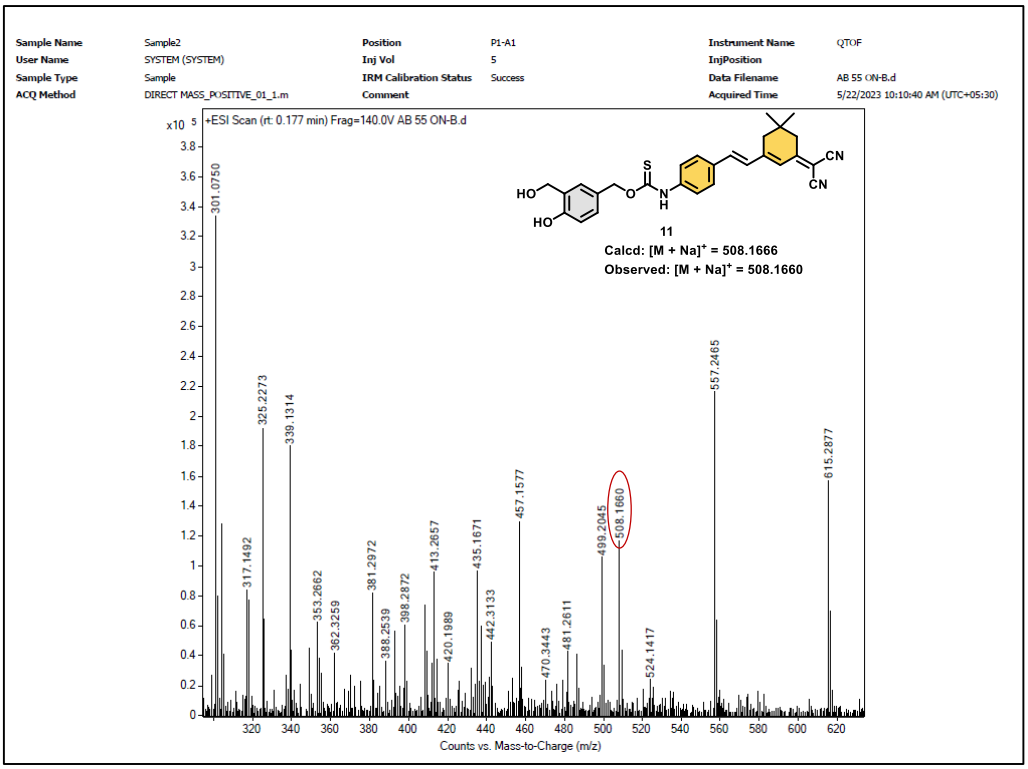

Figure S5. ESI-MS spectrum of the intermediate **11** in the reaction mixture of prodrug **DCF-HS** with H_2O_2 during HPLC analysis. ESI-MS (+ve) *m/z* calcd for $C_{28}H_{27}N_3NaO_3S$ $[M + Na]^+$ = 508.1666; obs = 508.1660.

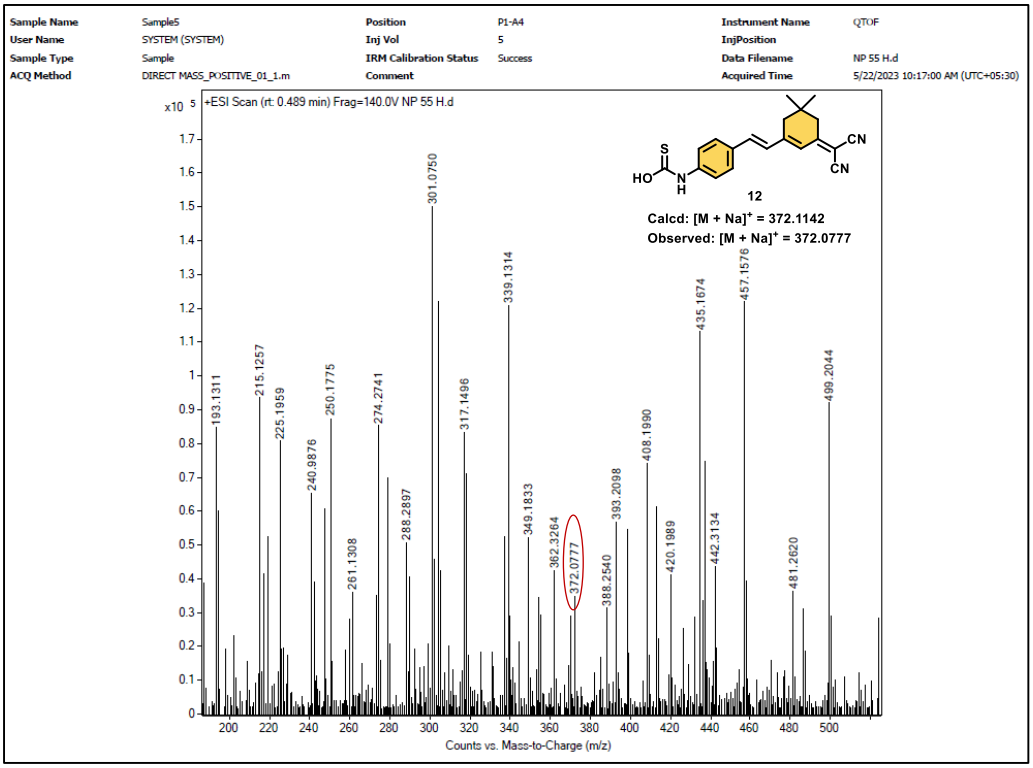

Figure S6. ESI-MS spectrum of the intermediate **12** in the reaction mixture of prodrug **DCF-HS** with H_2O_2 during HPLC analysis. ESI-MS (+ve) *m/z* calcd for $C_{20}H_{19}N_3NaOS$ $[M + Na]^+$ = 372.1142; obs = 372.0777.

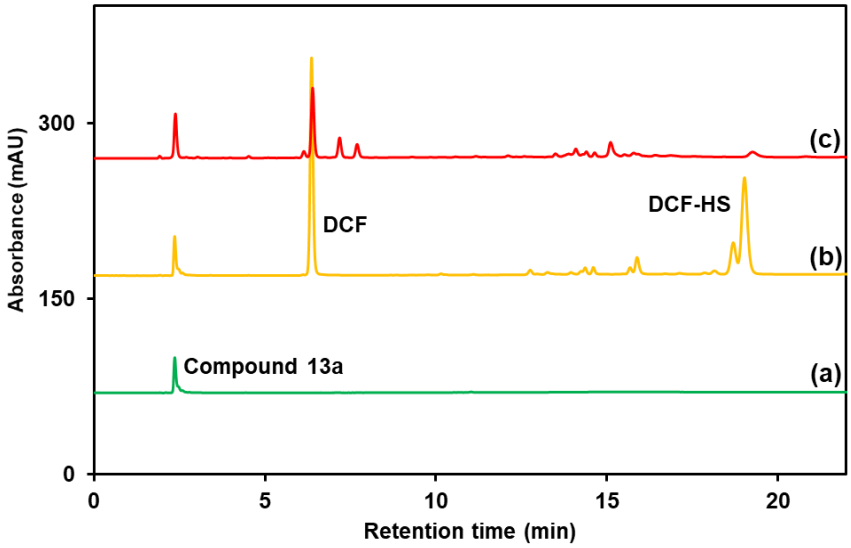

Figure S7. HPLC chromatograms for the reaction of **DCF-HS** (50 µM) with H_2O_2 (2.5 mM) and the release of by-product **13a**; Lanes: (a) pure compound **13a** (50 µM, 280 nm); (b) Mixture of pure **DCF-HS**, **DCF**, and compound **13a** (280 nm); (c) **DCF-HS** + H_2O_2 (t = 12 h, 280 nm).

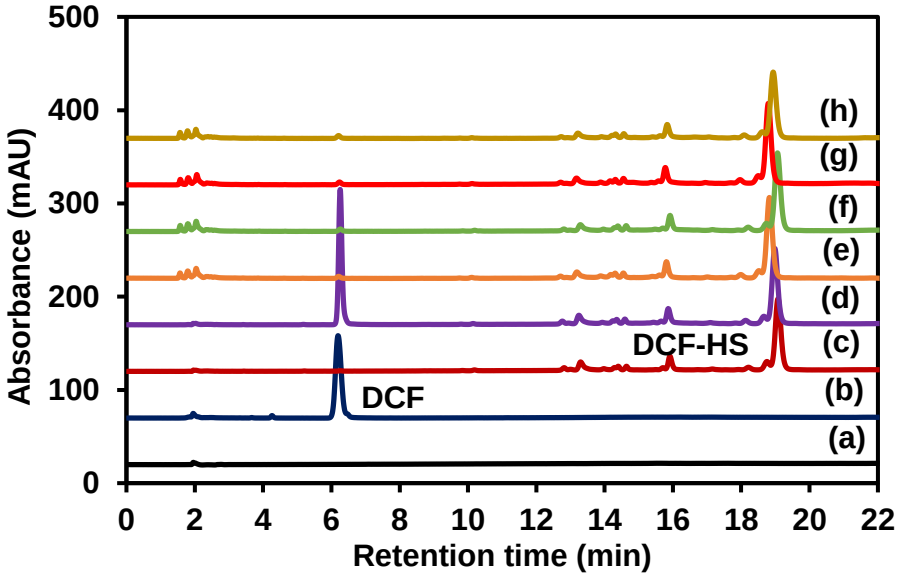

Figure S8. Reverse-phase HPLC chromatograms for the reaction of **DCF-HS** (50 µM) with esterase (5 U/mL); Lanes: (a) PBS (pH = 7.4, 254 nm); (b) pure **DCF** (50 µM, 280 nm); (c) pure **DCF-HS** (50 µM, 280 nm); (d) **DCF-HS** and **DCF** (50 µM, 280 nm); (e) **DCF-HS** + Esterase (t = 2 h, 280 nm); (f) **DCF-HS** + Esterase (t = 6 h, 280 nm); (g) **DCF-HS** + Esterase (t = 10 h, 280 nm); (h) **DCF-HS** + Esterase (t = 24 h, 280 nm).

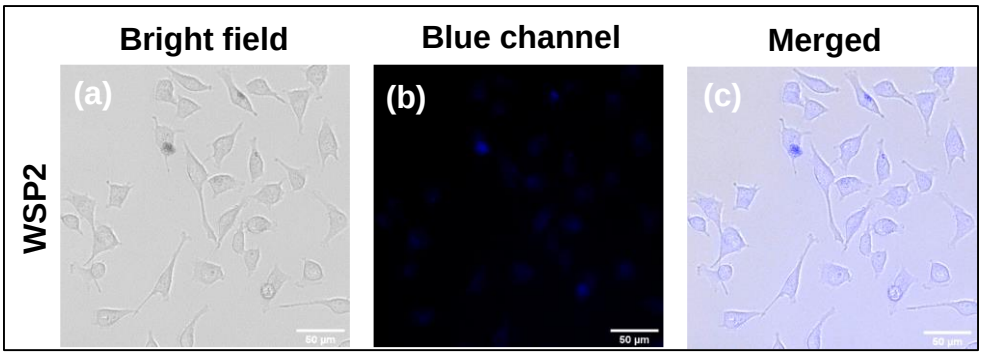

Figure S9. Fluorescence microscopy images (bright field, blue channel, and merged) of HeLa cells for the H_2S-selective turn-on fluorogenic probe **WSP2** (5 μM) for estimating the endogenous level of H_2S in HeLa cells. Scale bar: 50 μm.

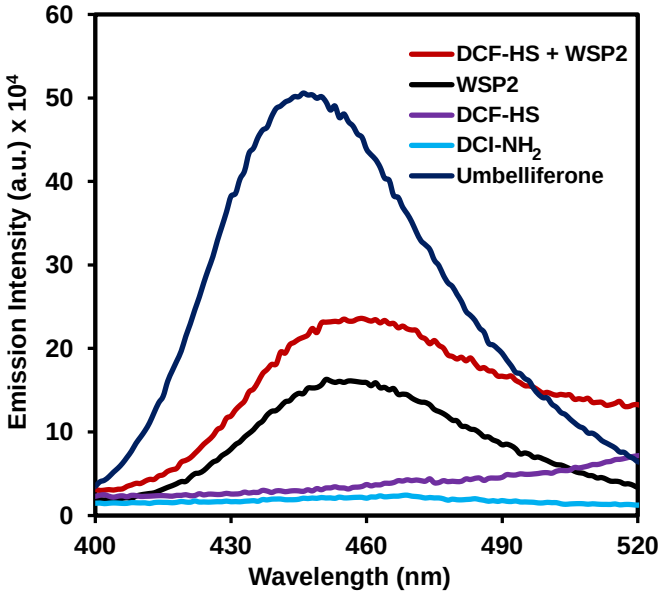

Figure S10. Fluorescence emission studies for detecting released H_2S from **DCF-HS** using the H_2S-selective probe **WSP2**. The prodrug **DCF-HS** (50 μM) was treated with **WSP2** (10 μM) in the presence of H_2O_2 (100 μM) and CA (50 μg/mL) in PBS (20 mM, pH = 7.4, with 2% DMSO, v/v) with an incubation of 12 h. The excitation wavelength was 322 nm with a slit width = 3/3. The emission intensity of pure **WSP2** (10 μM), umbelliferone (0.08 μM), and **DCI-NH$_2$** (50 μM) was measured under identical conditions.

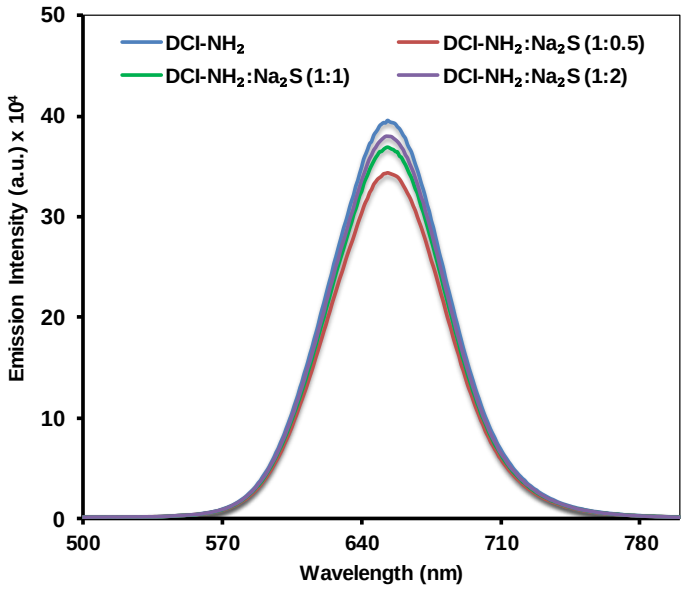

Figure S11. Fluorescence emission of **DCI-NH$_2$** (5 µM) in the absence and presence of a variable concentration (2.5, 5, and 10 µM) of $Na_2S.9H_2O$. The emission intensity was measured in PBS: DMSO system (1:1) after incubation for 60 min.

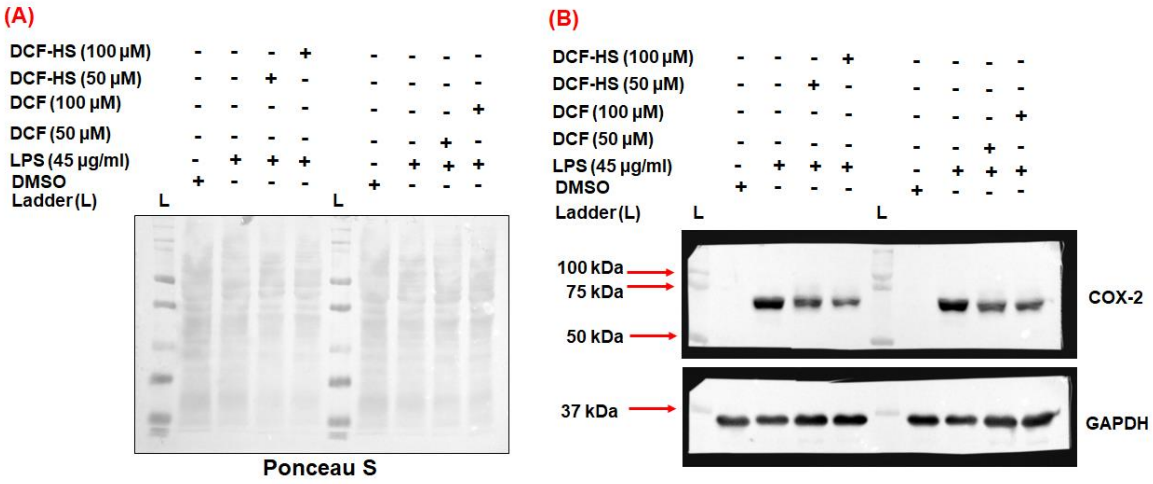

Figure S12. (A) Image of Ponceau S staining confirming the transfer of proteins on the nitrocellulose membrane from 12% SDS-PAGE gel before the final western blot images. (B) Uncropped raw Western blots for estimating COX-2 and GAPDH levels expression in LPS-induced macrophage cells (RAW 264.7) in the presence of **DCF-HS** and **DCF**.

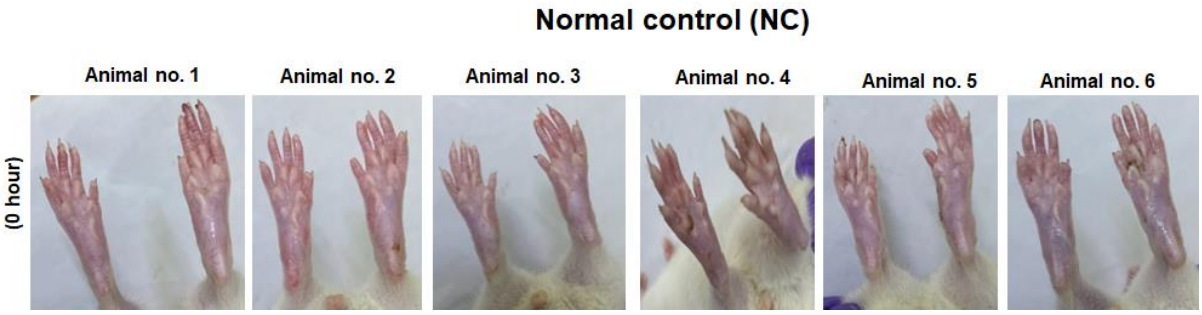

Figure S13. Image of the hind paw of the normal control (NC) group animals at 0 h.

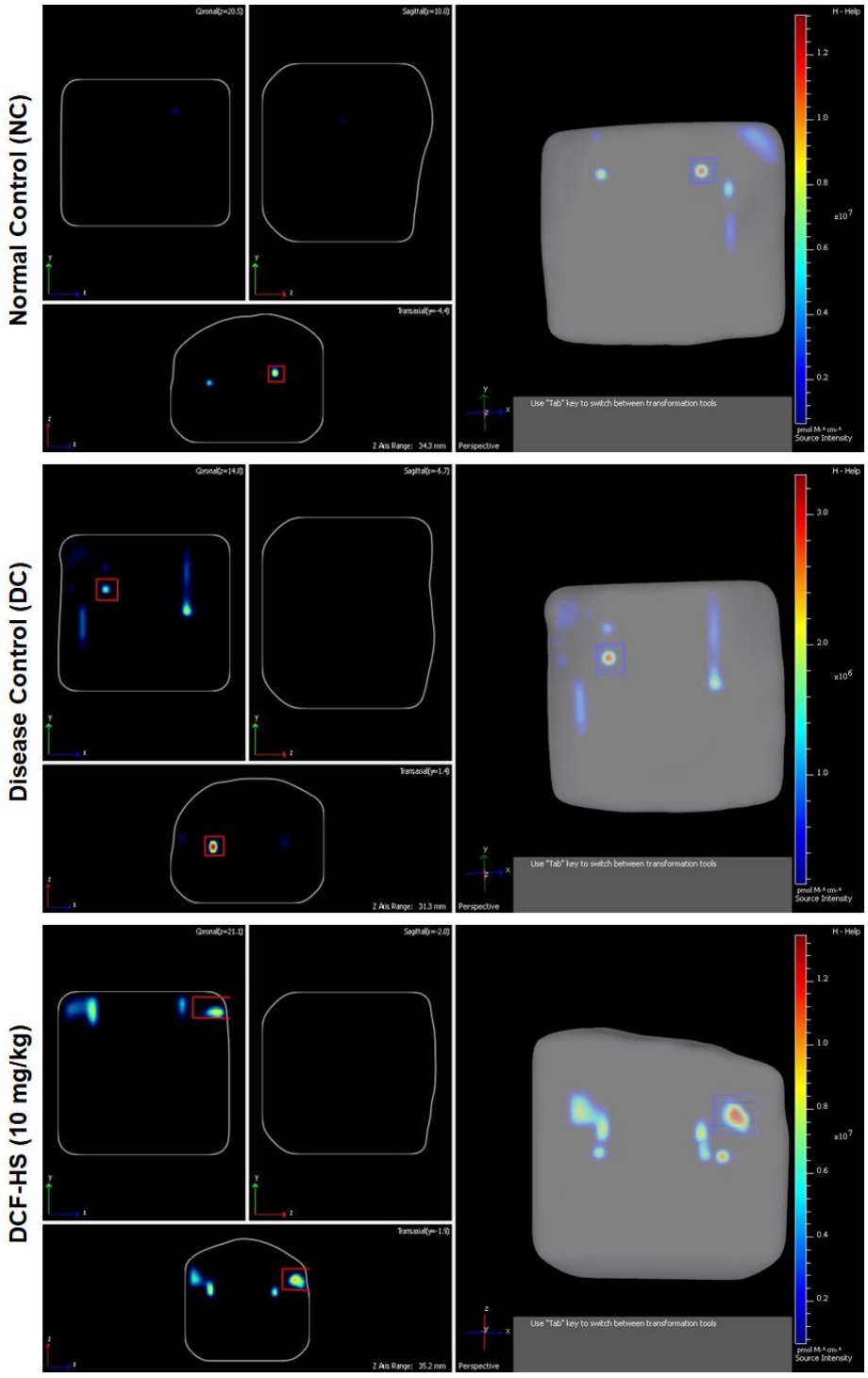

Figure S14. IVIS imaging in 3D in the trans-fluorescence mode to estimate released fluorescence intensity from **DCF-HS** compared to normal control and disease control Ex/Em: 480/660 nm.

NMR spectra of the synthesized compounds

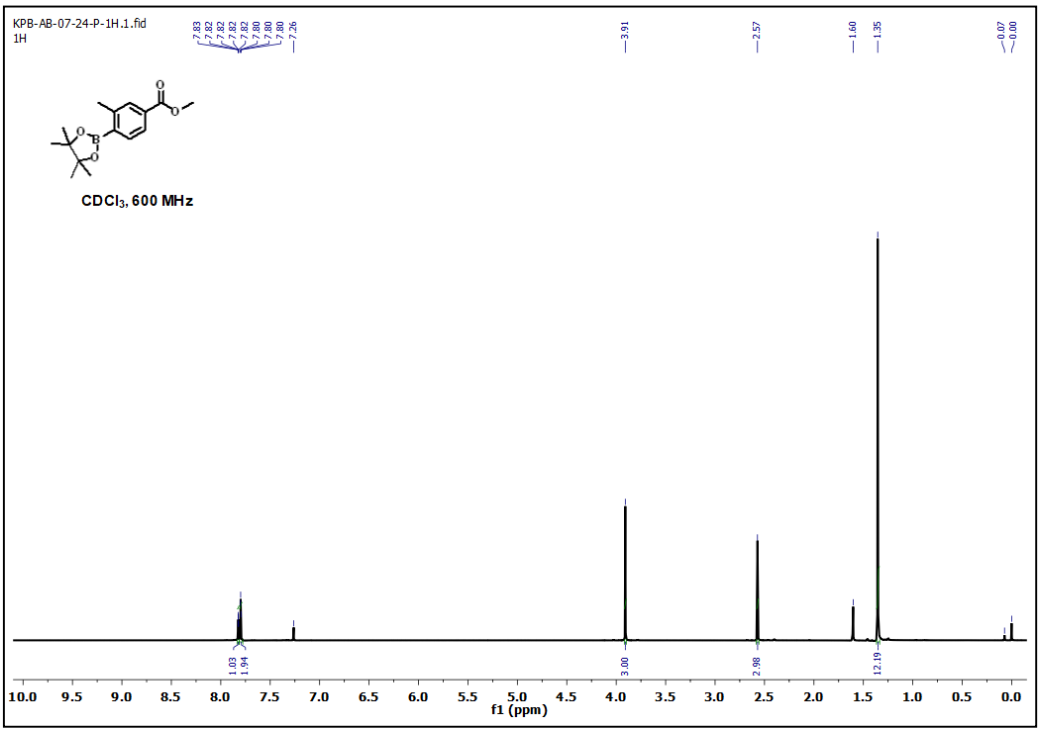

Figure S15. ^{1}H NMR spectrum ($CDCl_3$, 600 MHz) of compound **2**.

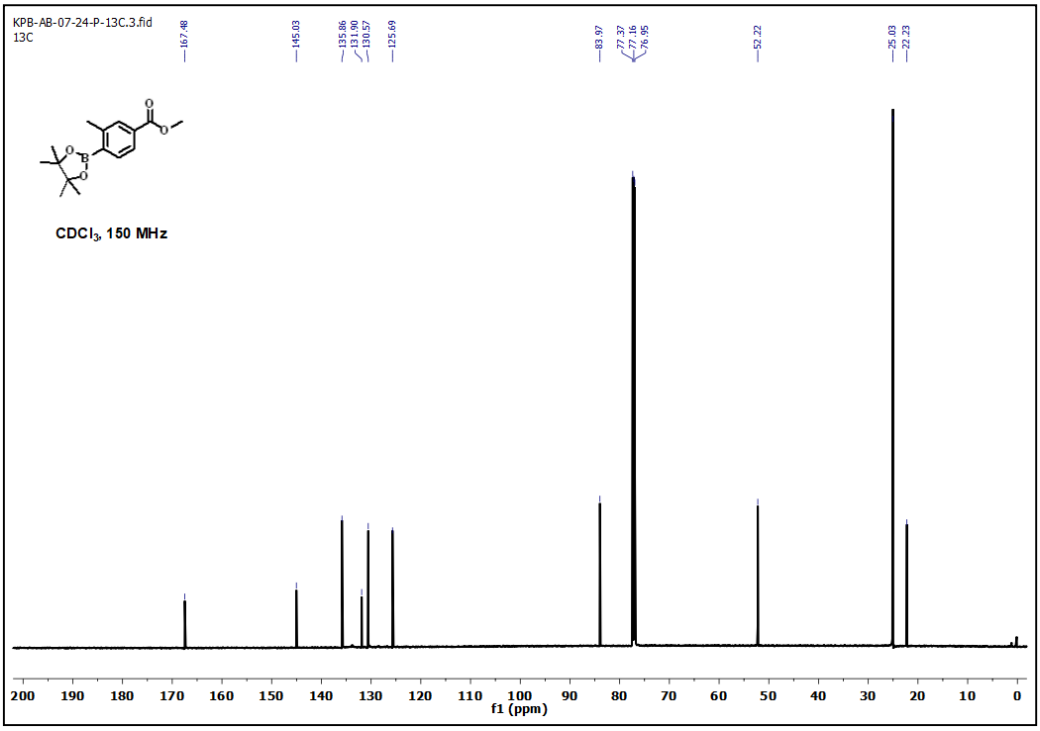

Figure S16. ^{13}C NMR spectrum ($CDCl_3$, 150 MHz) of compound **2**.

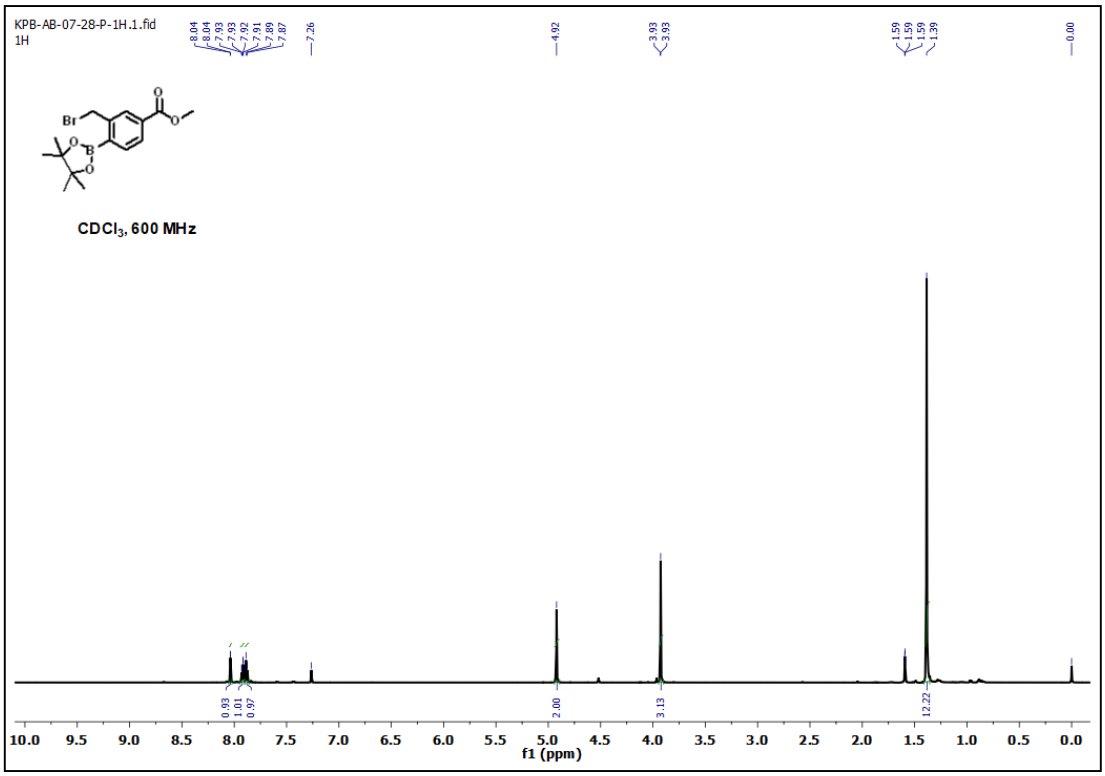

Figure S17. ^{1}H NMR spectrum ($CDCl_3$, 600 MHz) of compound **3**.

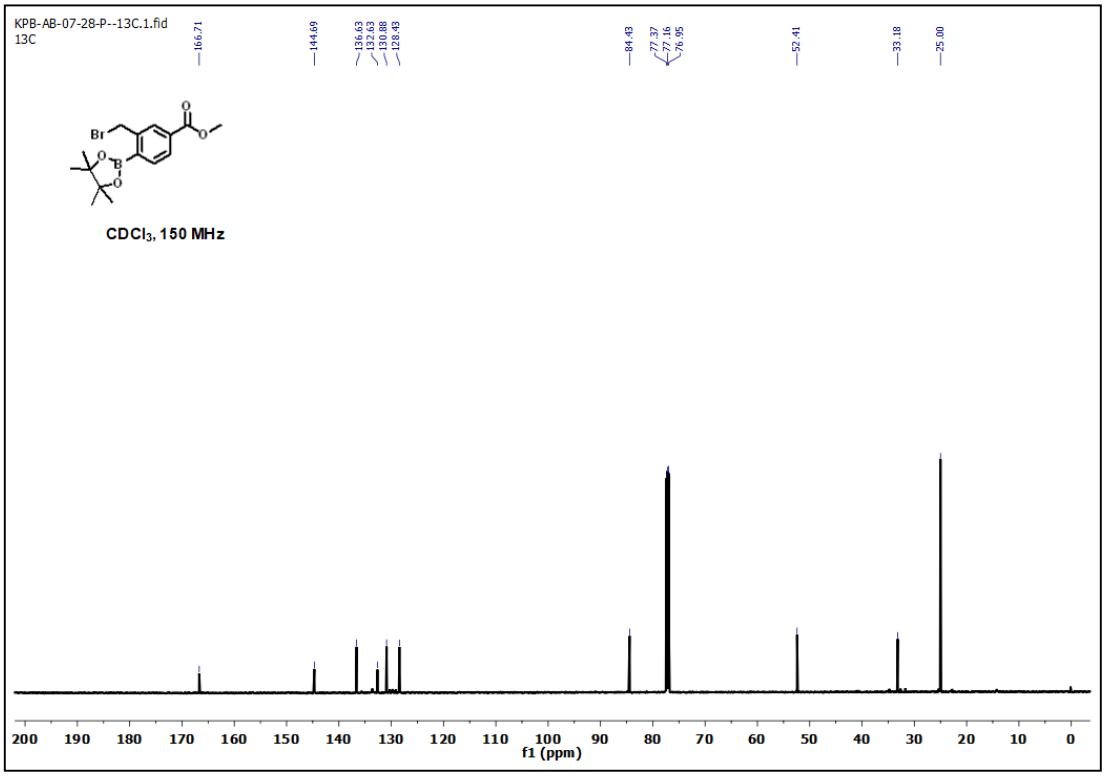

Figure S18. ^{13}C NMR spectrum ($CDCl_3$, 150 MHz) of compound **3**.

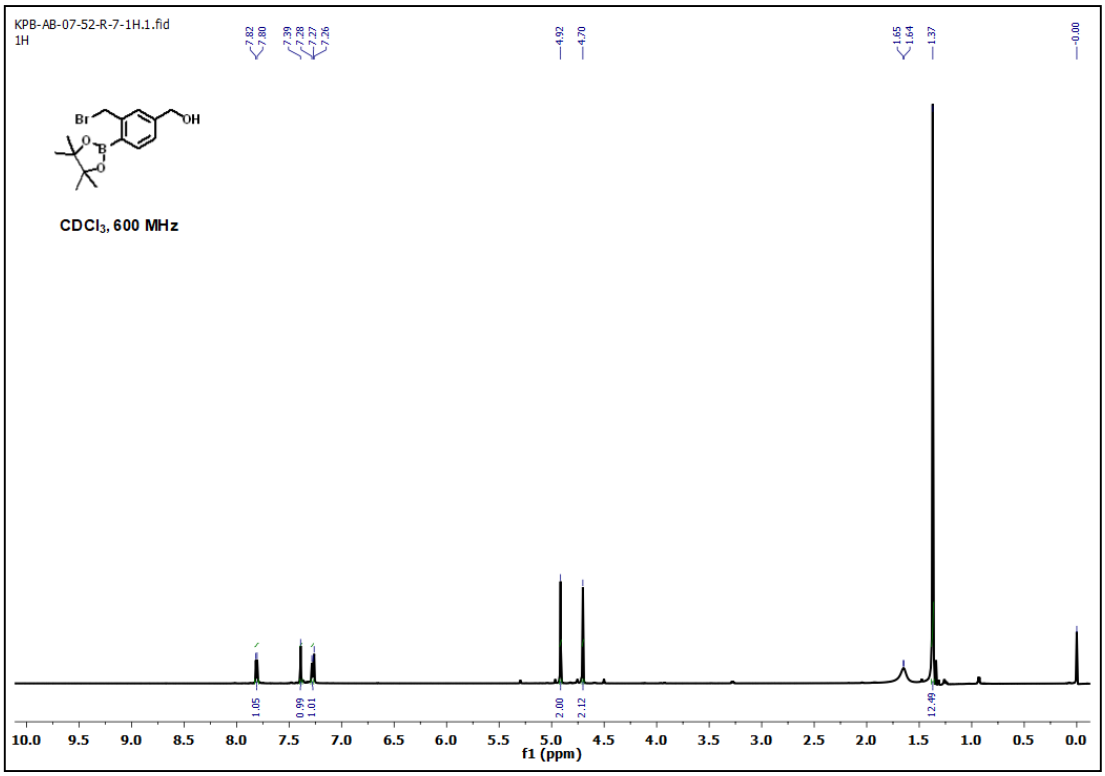

Figure S19. ^{1}H NMR spectrum ($CDCl_3$, 600 MHz) of compound **4**.

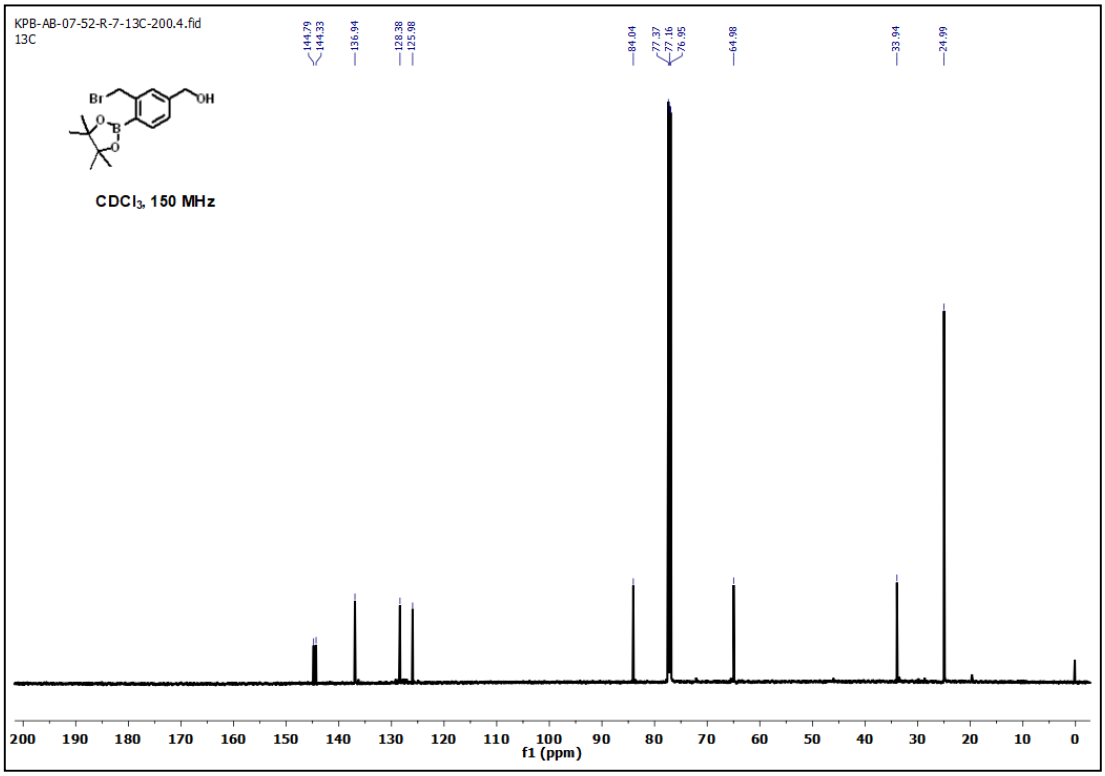

Figure S20. ^{13}C NMR spectrum ($CDCl_3$, 150 MHz) of compound **4**.

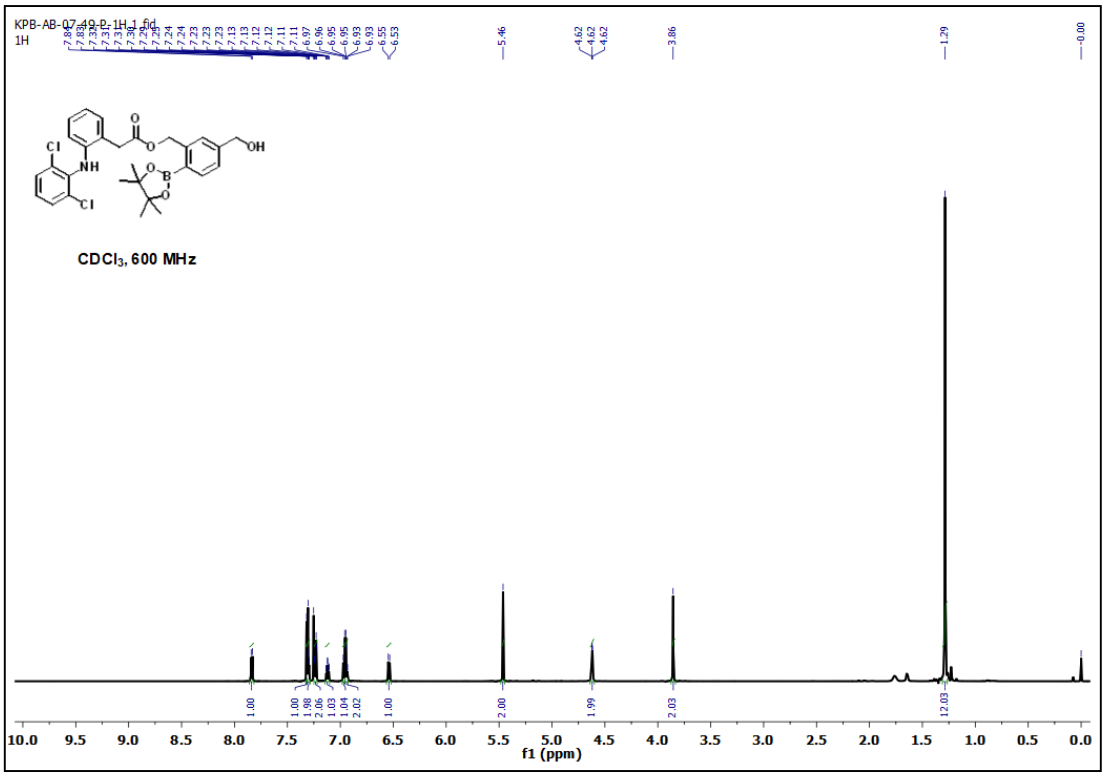

Figure S21. ^{1}H NMR spectrum ($CDCl_3$, 600 MHz) of compound **5**.

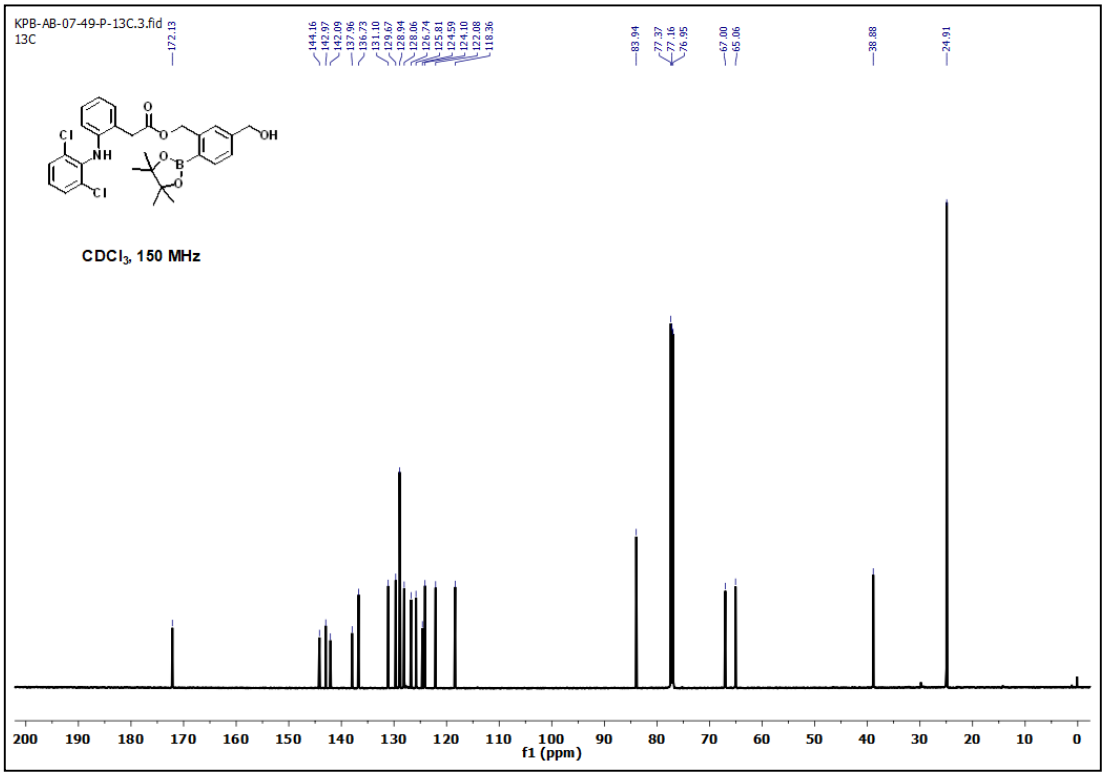

Figure S22. ^{13}C NMR spectrum ($CDCl_3$, 150 MHz) of compound **5**.

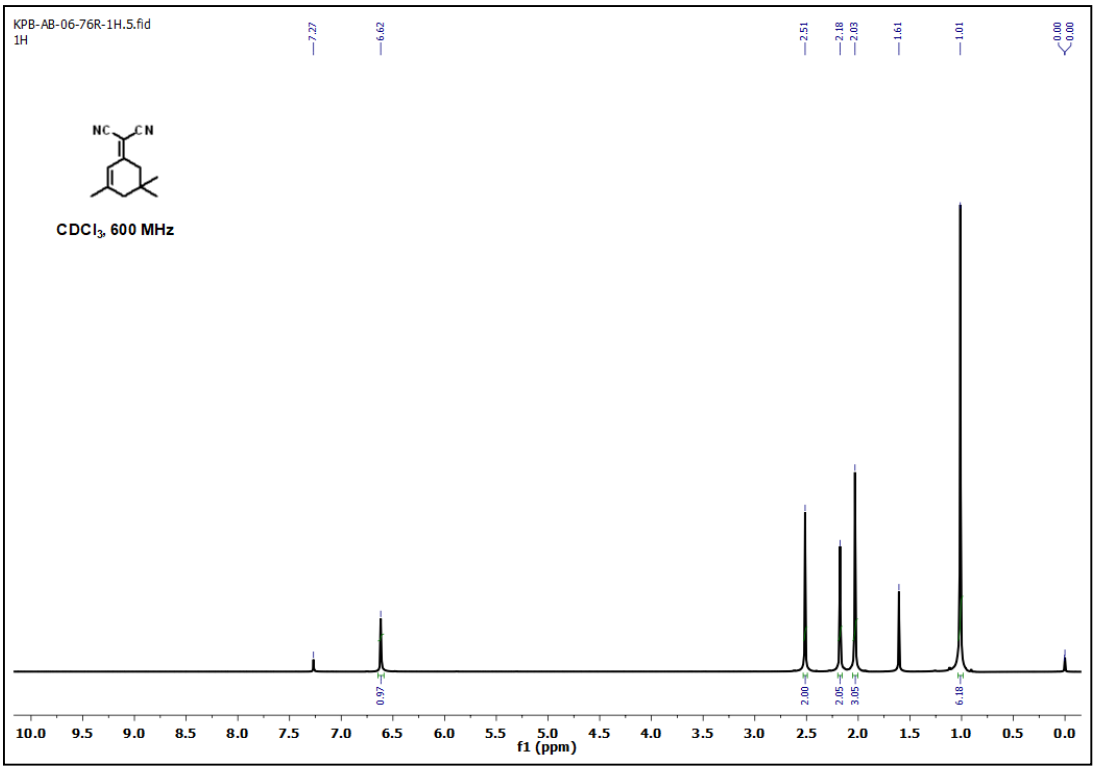

Figure S23. ^{1}H NMR spectrum ($CDCl_3$, 600 MHz) of compound **7**.

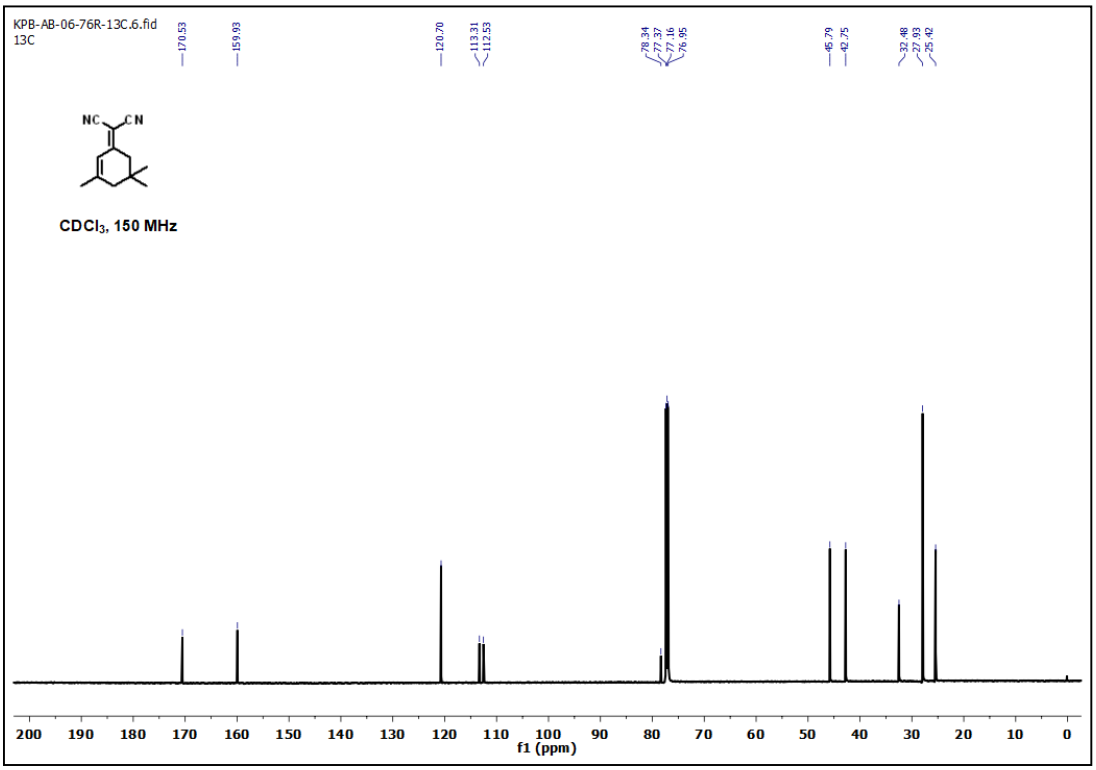

Figure S24. ^{13}C NMR spectrum ($CDCl_3$, 150 MHz) of compound **7**.

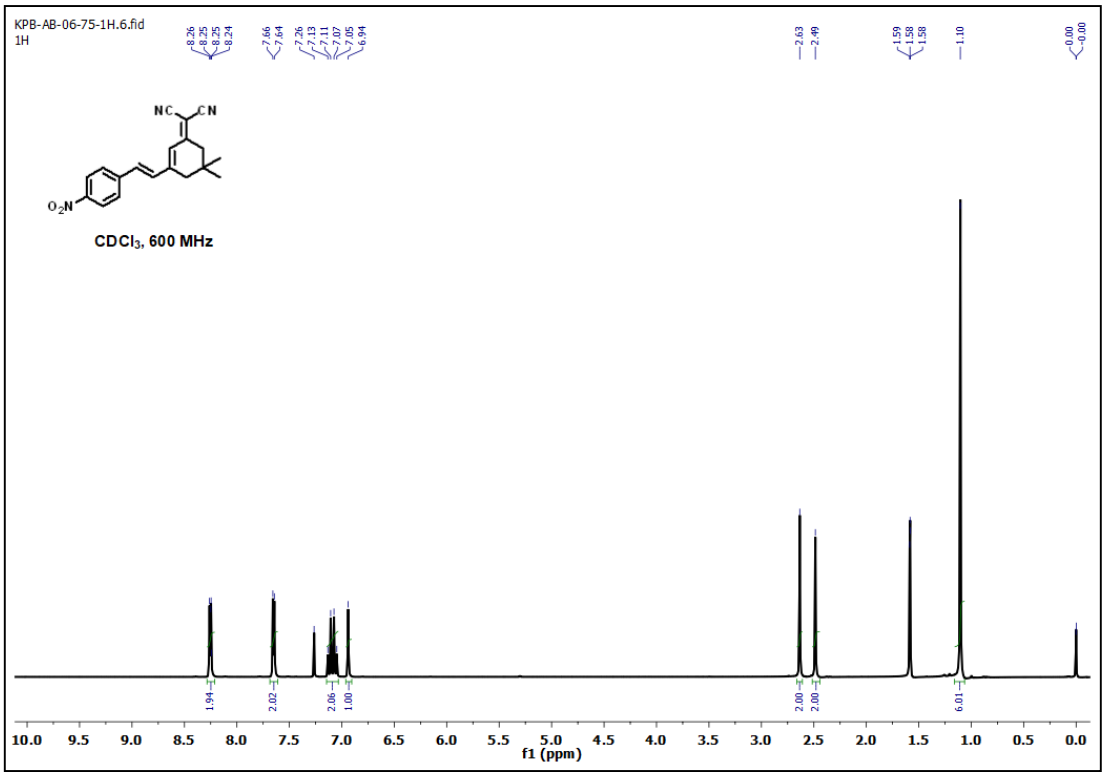

Figure S25. ^{1}H NMR spectrum ($CDCl_3$, 600 MHz) of compound **8**.

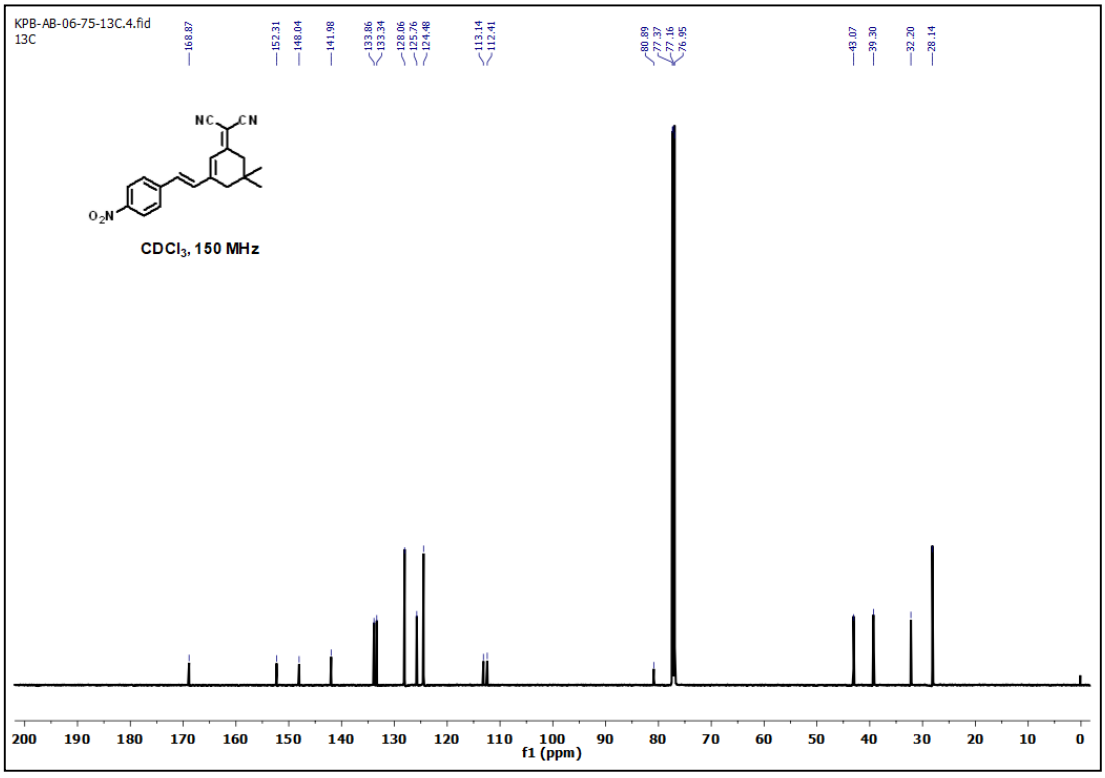

Figure S26. ^{13}C NMR spectrum ($CDCl_3$, 150 MHz) of compound **8**.

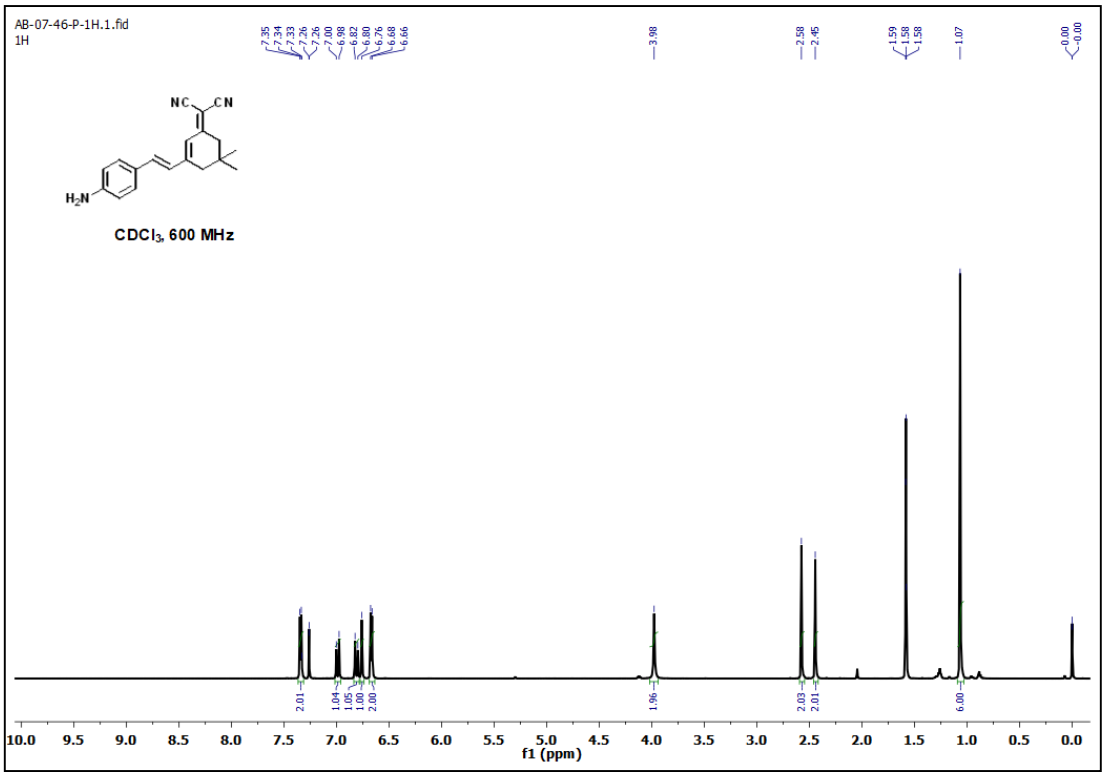

Figure S27. ^{1}H NMR spectrum ($CDCl_3$, 600 MHz) of compound **DCI-NH$_2$**.

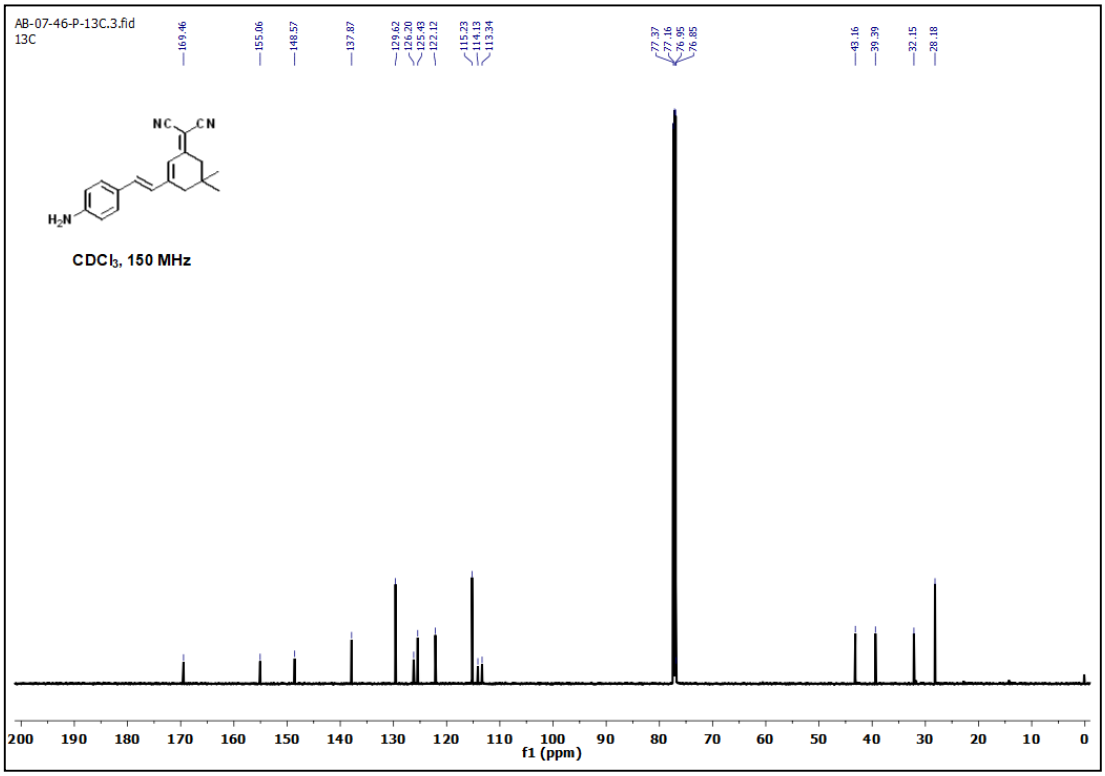

Figure S28. ^{13}C NMR spectrum ($CDCl_3$, 150 MHz) of compound **DCI-NH$_2$**.

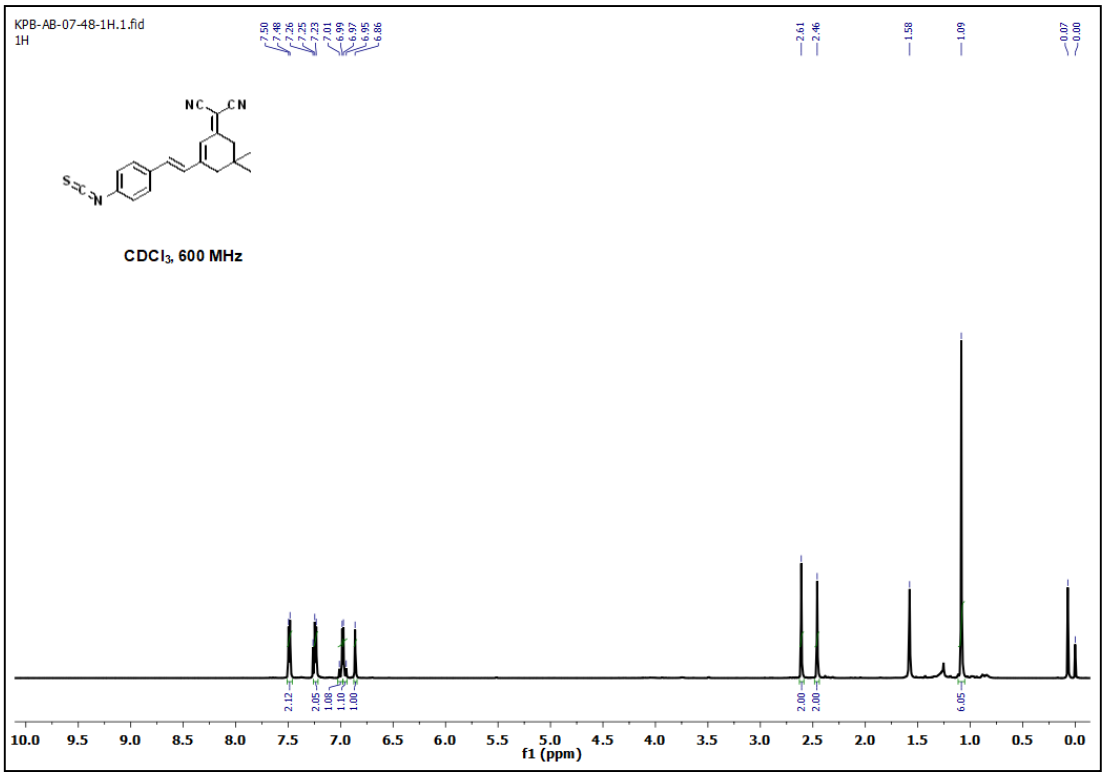

Figure S29. ^{1}H NMR spectrum ($CDCl_3$, 600 MHz) of compound **9**.

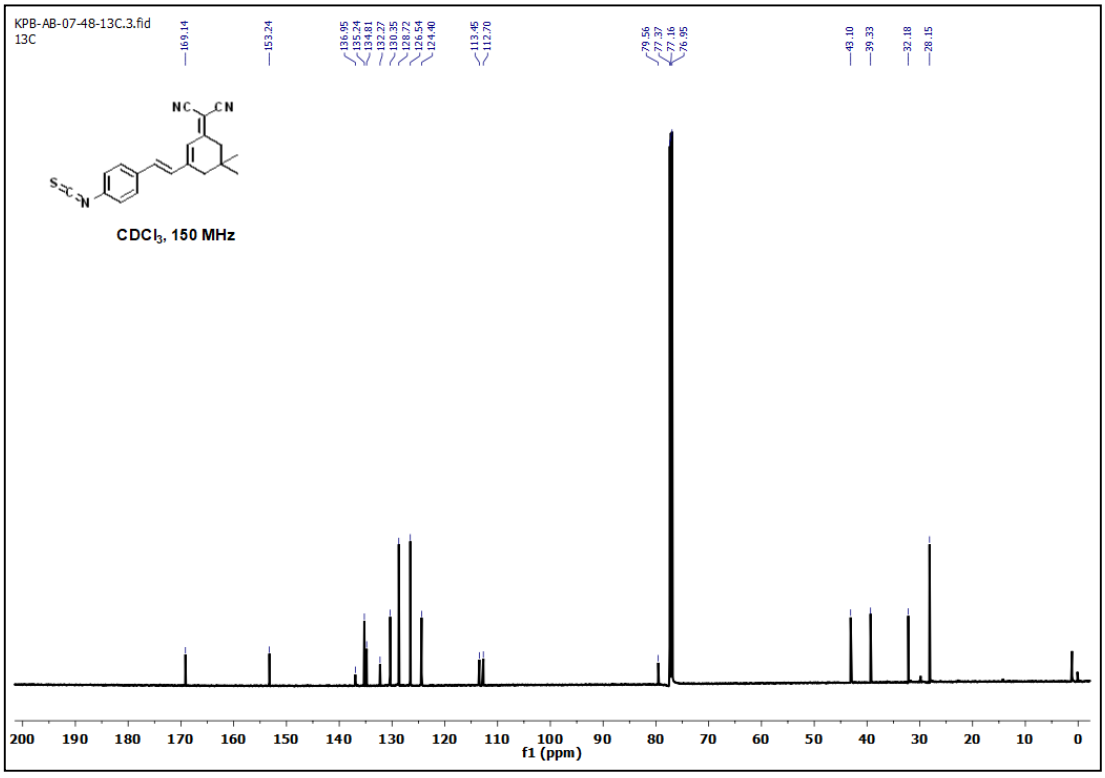

Figure S30. ^{13}C NMR spectrum ($CDCl_3$, 150 MHz) of compound **9**.

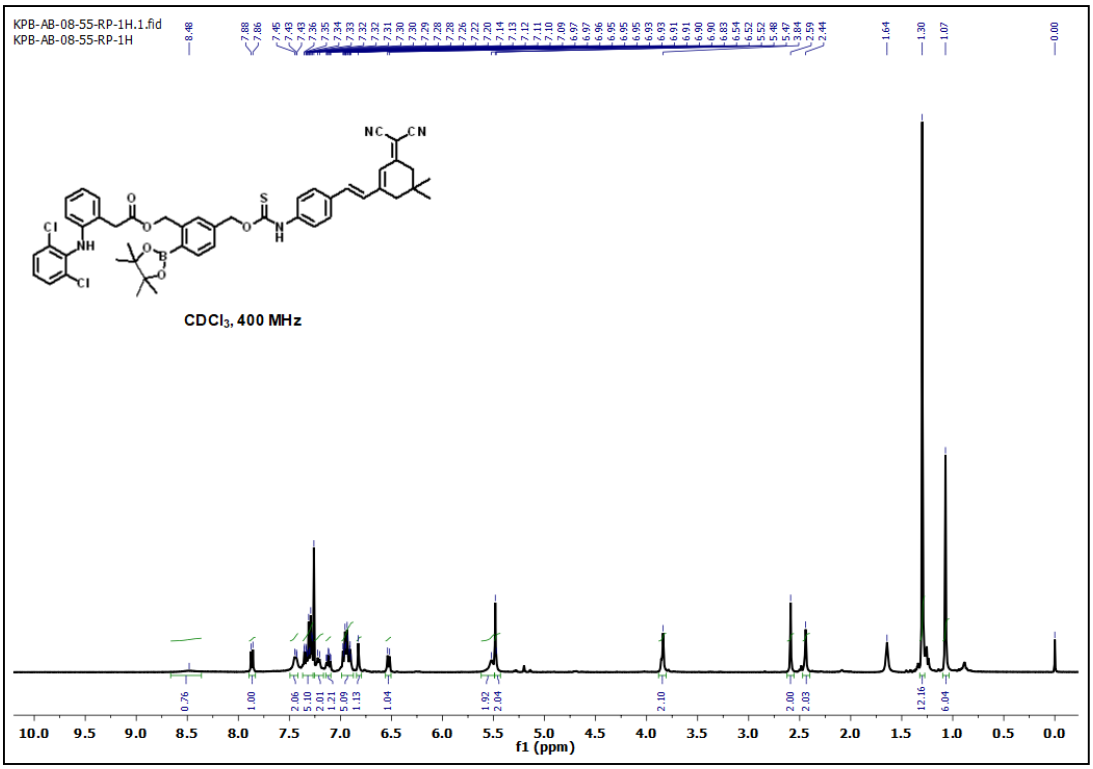

Figure S31. ^{1}H NMR spectrum ($CDCl_3$, 400 MHz) of compound **DCF-HS**.

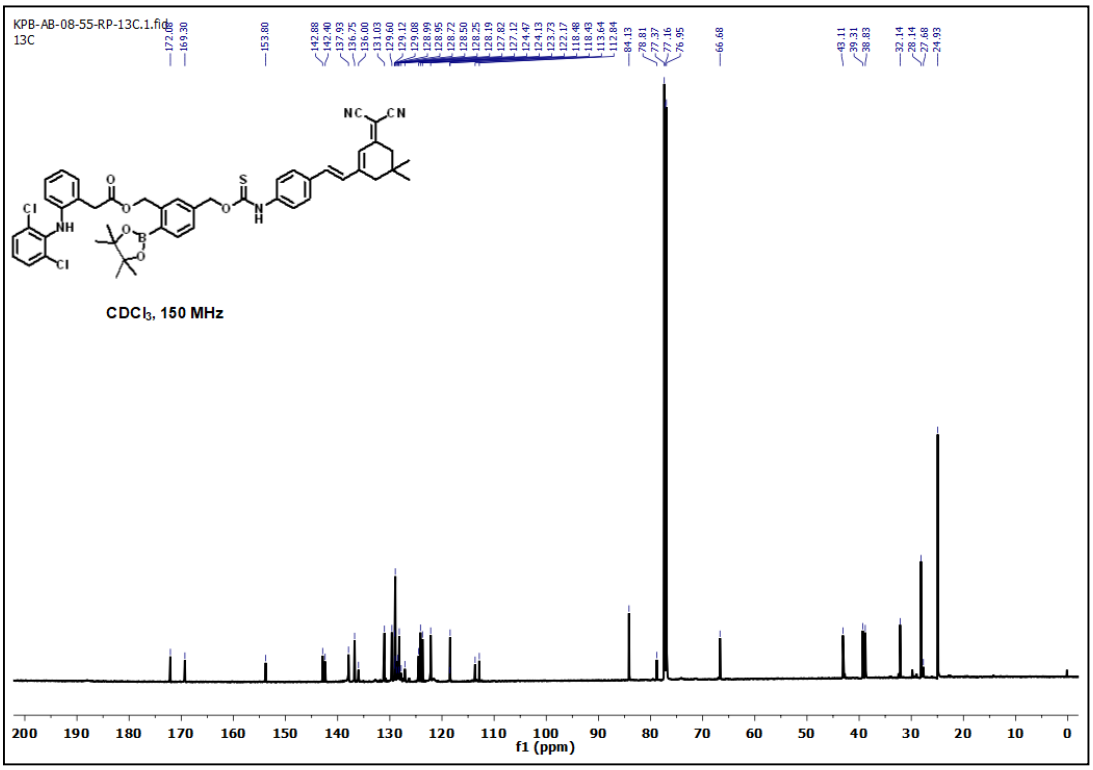

Figure S32. ^{13}C NMR spectrum ($CDCl_3$, 150 MHz) of compound **DCF-HS**.

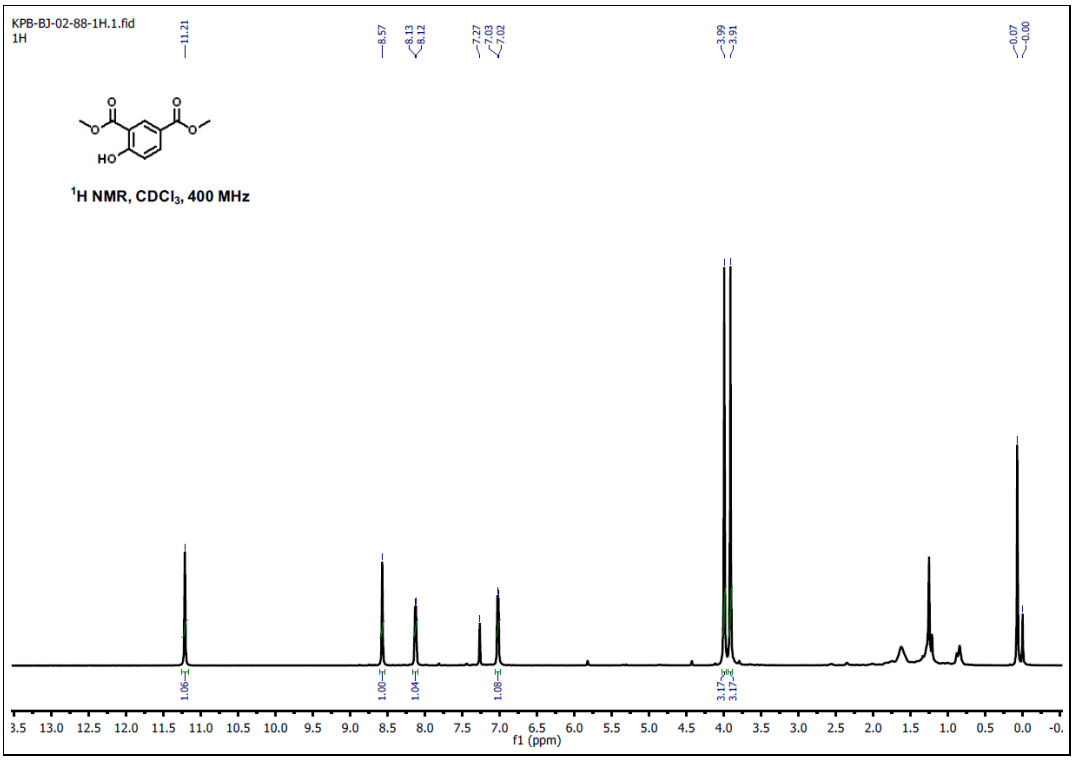

Figure S33. ^{1}H NMR spectrum ($CDCl_3$, 400 MHz) of compound **15**.

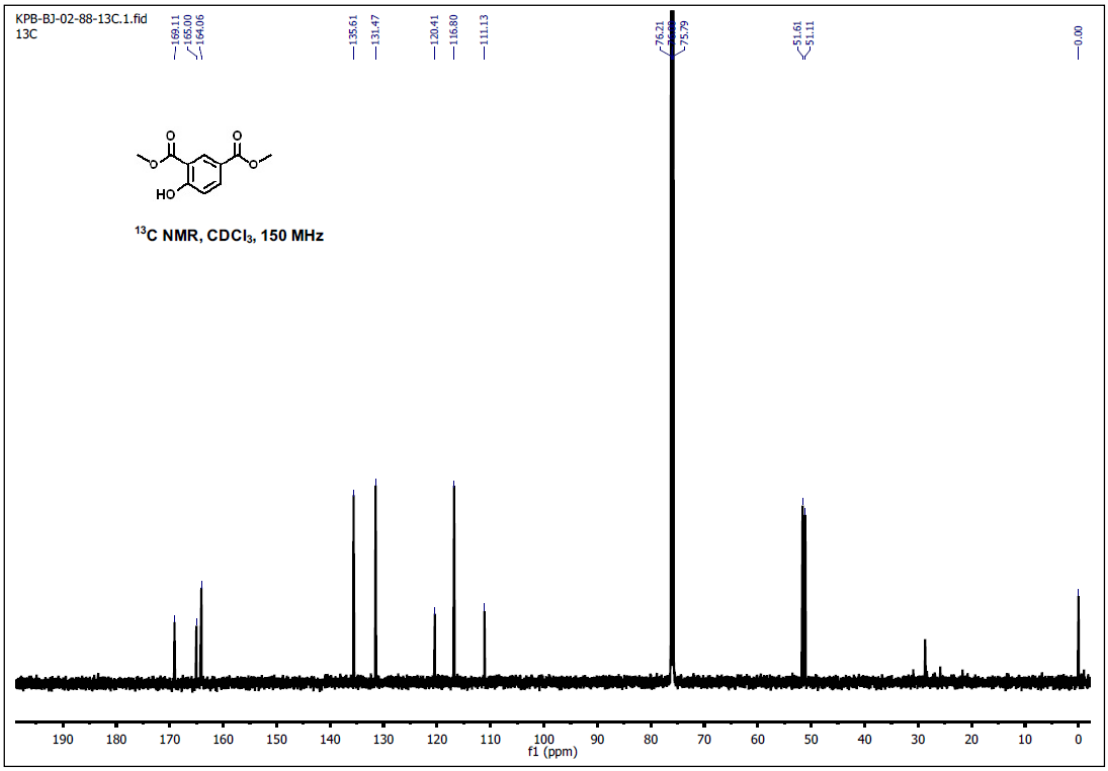

Figure S34. ^{13}C NMR spectrum ($CDCl_3$, 150 MHz) of compound **15**.

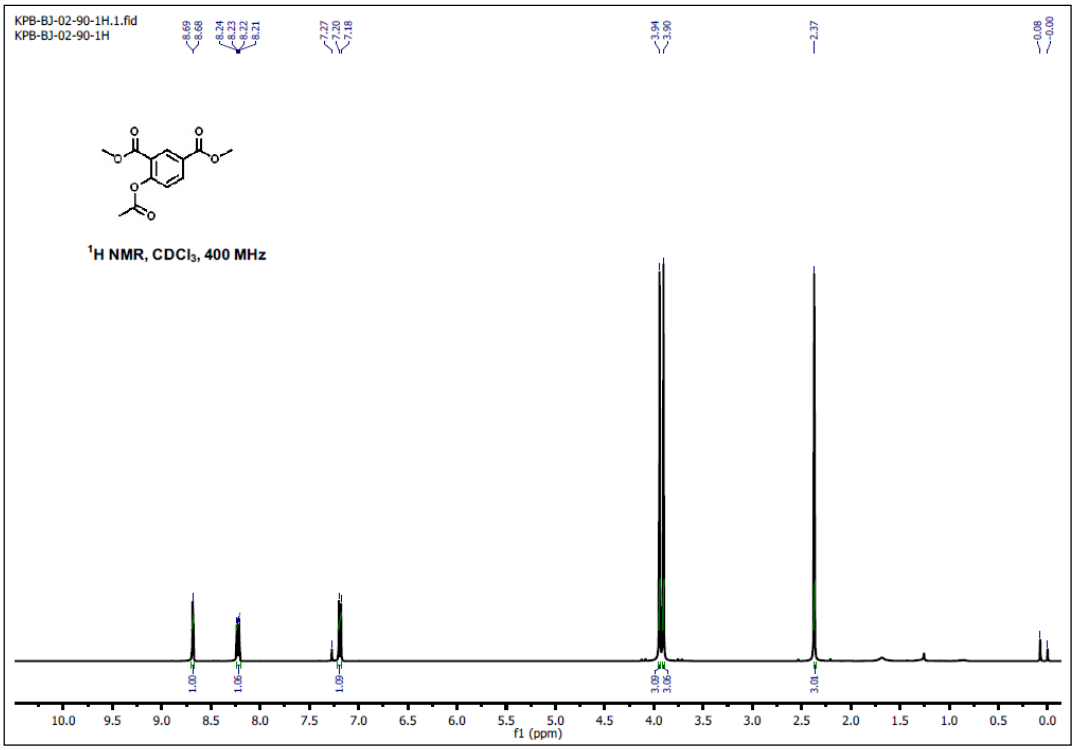

Figure S35. ^{1}H NMR spectrum ($CDCl_3$, 400 MHz) of compound **16**.

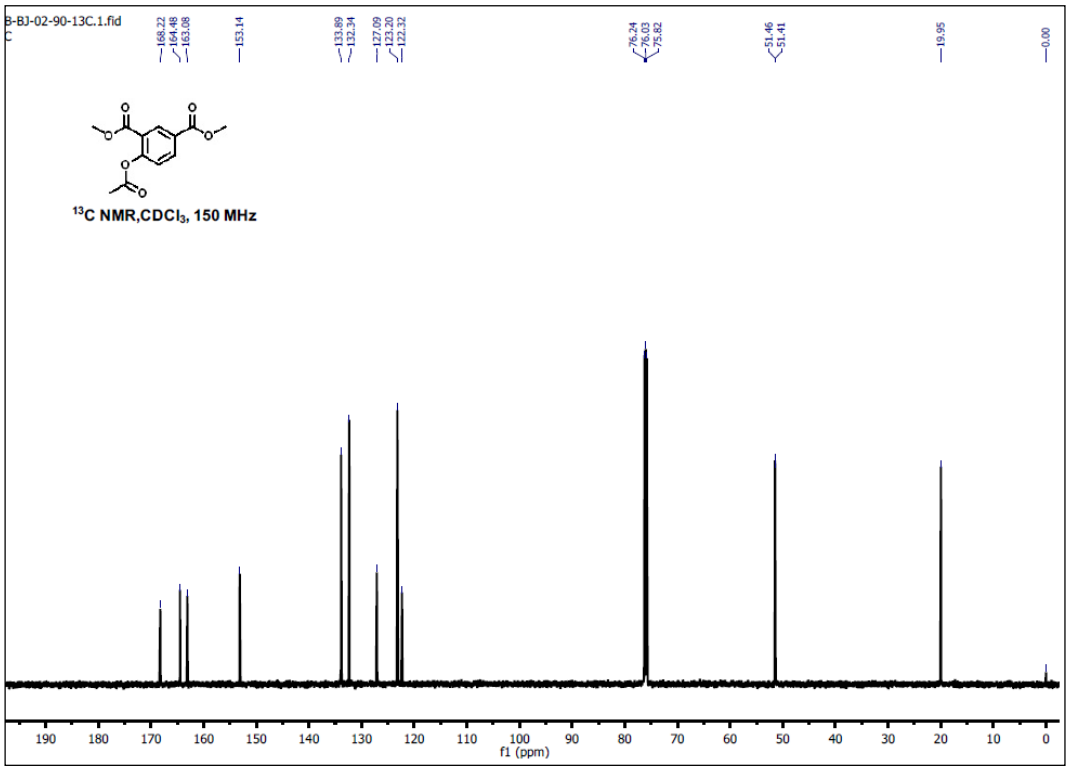

Figure S36. ^{13}C NMR spectrum ($CDCl_3$, 150 MHz) of compound **16**.

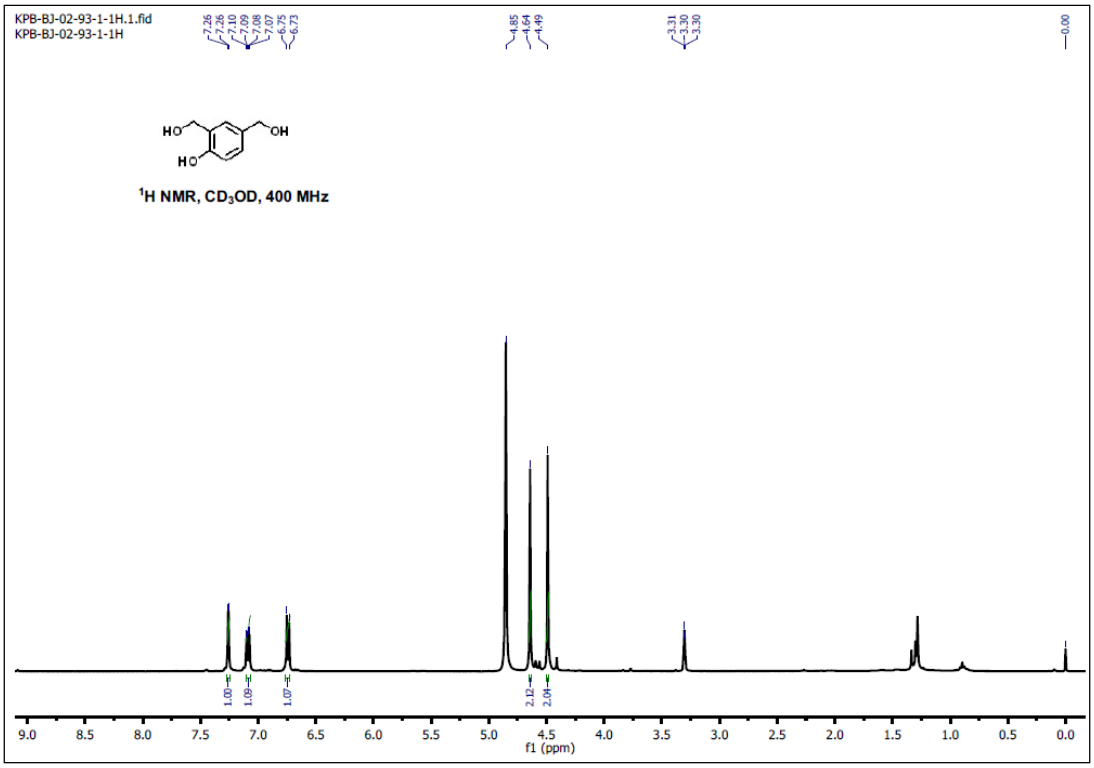

Figure S37. ^{1}H NMR spectrum (CD$_3$OD, 400 MHz) of compound **13a**.

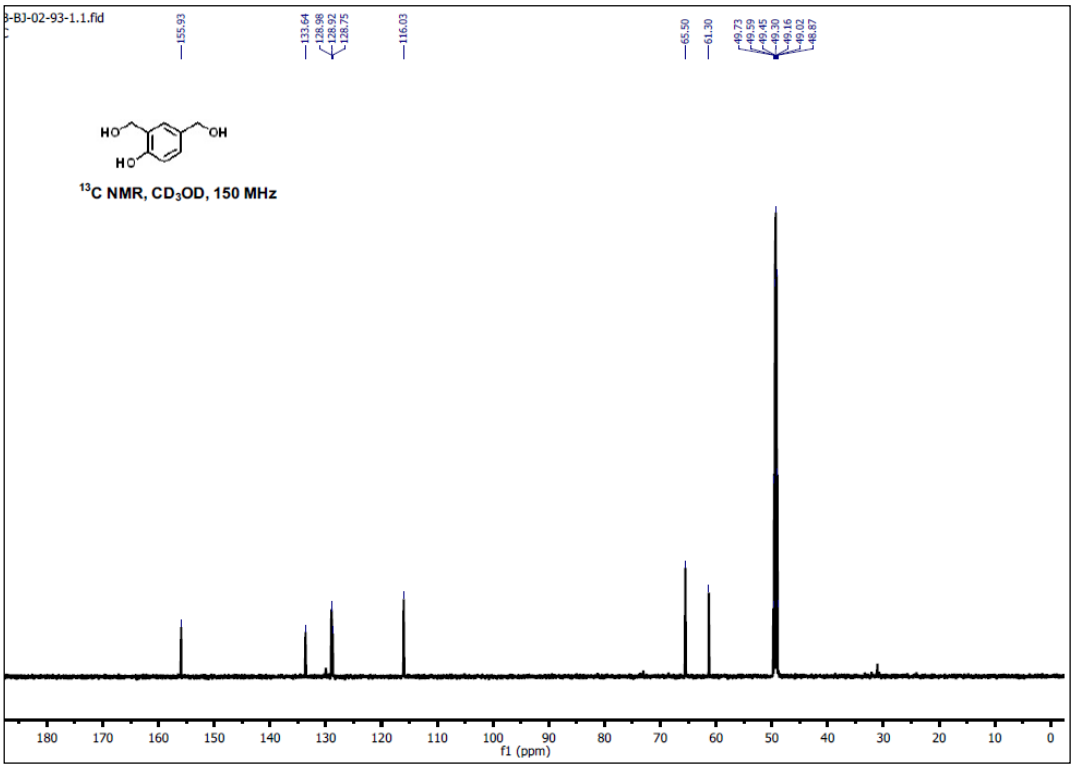

Figure S38. ^{13}C NMR spectrum (CD$_3$OD, 150 MHz) of compound **13a**.

References

1. J. H. Freeman, *J Am Chem Soc*, 1952, **74**, 6257-6260.
2. J. Rehbein, S. Leick and M. Hiersemann, *J Org Chem*, 2009, **74**, 1531-1540.
3. C. Ding, Y. Yu, Q. Yu, Z. Xie, Y. Zhou, J. Zhou, G. Liang and Z. Song, *ChemCatChem*, 2018, **10**, 5397-5401.
4. T. Fukuda, E. Matsumoto, S. Onogi and Y. Miura, *Bioconjugate Chem*, 2010, **21**, 1079-1086.